Vibrational Spectra of CO_2-Electron Donor−Acceptor Complexes from ab Initio

Y. Danten,* T. Tassaing, and M. Besnard

Laboratoire de Physico-Chimie Moléculaire (U.M.R C.N.R.S 5803), Université Bordeaux I, 351, Cours de la Libération, 33405 Talence, France

Received: July 11, 2002

In this paper, we investigated the 1:1 EDA complexes of CO_2 formed with alcohols, namely, methanol and ethanol (sp^3 O-donating atom), and with acetone (sp^2 O-donating atom) in light of ab initio calculations. The interaction energy and the geometry of the complexes have been evaluated with the Moller−Plesset perturbation theory at the second-order level (MP2) using Dunning's basis sets. The predicted structures are found to be rather similar compared with the calculations at the SCF/3-21G* level reported by Jamroz et al. (Jamroz, M. H.; Dobrowolski, J. C.; Bajdor, K.; Borowiak, M. A. *J. Mol. Struct.* **1995**, *349*, 9.). Nevertheless, the stabilization energies are found in our work to be 2 to 2.5 times lower including electron correlation. In addition, we have analyzed the vibrational spectra of these EDA complexes. In particular, we emphasized the splitting of the ν_2 bending mode of CO_2 and the ν_S(OH) stretching mode of alcohols or the antisymmetric ν_a(CCC) and symmetric ν_s(CO) stretching modes of acetone. Finally, the shift and the IR and Raman intensity variations under the complex formation are discussed and compared with infrared absorption and Raman experimental measurements.

1. Introduction

During the last two decades, the understanding of interactions of carbon dioxide (CO_2) with organic and/or inorganic compounds has been the subject of a large body of experimental and theoretical studies.[1−17] Now, it is well established that the CO_2 molecule can play either the role of proton acceptor (involving a hydrogen-bond interaction) or the role of electron acceptor or electron donor according to the nature of the organic molecule.

In the presence of Lewis bases such as water,[3−6,12] alcohols (methanol, ethanol),[3,4,10,11] ketones,[1,12] amines, and amides,[3−6] the acidity of the CO_2 molecule (through the carbon atom) leads to the formation of electron donor−acceptor (EDA) complexes. This Lewis acid−base interaction affects the intramolecular bonds differently, hence the strength of the internal force constants, leading to strong perturbations of the vibrational spectra of each moiety. For this reason, infrared absorption and Raman scattering constitute powerful tools to probe such interactions.

The combination of IR spectroscopic measurements with ab initio computations has proven to be of great interest in the study of EDA complex formation in gaseous and liquid phases. As a matter of fact, spectroscopic[4,14,15] and theoretical chemistry evidence[3,5,6,13] leads us to conclude that molecules having a functional electron-donating center (at least a lone electron pair) favorably interact with CO_2. In this context, the study of J. Dobrowolsky et al. has provided evidence of the formation of EDA complexes for CO_2 dissolved in a number of liquid organic solvents on the basis of infrared measurements[4] combined with ab initio calculations.[3] This study enables us to show that CO_2 complexes formed with sp^3 O-donating atoms (H_2O, alcohols, ethers) are more stable than complexes involving sp^2 O-donating atoms (aldehydes, ketones).

More recently, such studies have been extended to CO_2 EDA complexes in supercritical fluids. This is explained because supercritical (SC) CO_2 is widely used as a solvent in a large number of industrial applications (extraction, materials processing, polymers fractionation, etc.[18−22]) and offers easy operating conditions (low critical parameters). However, even under supercritical conditions, the solvating power of CO_2 still remains limited for highly polar species and high molecular weight solutes. For this reason, SC CO_2 is used with a cosolvent, generally an alcohol or a ketone, to improve the solvation of solutes. Clearly, the study of the CO_2−solute (cosolvent) interactions is of crucial interest to the understanding of the solvation process. Few vibrational spectroscopic studies have been carried out on binary mixtures of alcohols or ketones in SC CO_2. Studies by FTIR measurements and Raman scattering of alcohols diluted in SC CO_2 have revealed the formation of weak EDA complexes between CO_2 and alcohols (methanol, ethanol).[23−27] Evidence of such EDA interactions has been also provided in the swelling process by SC CO_2 of polymers containing carbonyl groups.[1,12]

This paper is aimed at the study of 1:1 EDA complexes of CO_2 formed with alcohols, namely, methanol and ethanol (sp^3 O-donating atom), and with acetone (sp^2 O-donating atom). In our investigation, we have determined the structures and the stabilization energies of these CO_2 complexes and have analyzed their vibrational spectra. The latter point of view has been addressed with a particular emphasis on the splitting of the ν_2 bending mode of CO_2 and on the ν_S(OH) stretching mode of alcohols or on the antisymmetric ν_a(CCC) and symmetric ν_s(CO) stretching modes of acetone. We have also discussed the shift and the IR and Raman intensity variations associated with each internal mode under the complex formation. Finally, our ab initio spectral predictions have been compared with infrared absorption and Raman experimental measurements reported in the literature, as available, and also with our IR absorption spectra of alcohols and ketones dissolved in SC CO_2.

* Corresponding author. E-mail: y.danten@lpcm.u-bordeaux1.fr. Phone: 33-5-56-84-63-59. Fax: 33-5-56-84-84-02.

10.1021/jp021598v CCC: $22.00
Published on Web 11/06/2002

2. Methodology of Calculations

All the calculations reported in this paper have been carried out using the Gaussian 98 program.[28] The geometry of all the complexes investigated here and of their corresponding isolated moieties has been fully optimized at the second-order Moller−Plesset (MP2) level of perturbation theory[29] using the very tightest criterion of convergence. In rare troublesome cases, a very efficient method for helping convergence, the so-called Puley extrapolation procedure gdiis,[30] has been additionally implemented in the geometry optimization calculation of the complex considered. The optimized geometry computation was not subjected to a particular symmetry constraint except for isolated monomers (optimized in their molecular symmetry). The geometry calculations have been achieved using the correlation-consistent polarized valence double/triple-zeta basis sets proposed by Dunning and co-workers[31−33] as well as the augmented basis sets.[34] These basis sets are designated by their acronyms cc-pVTZ (valence triple) and aug-cc-pVDZ (augmented valence double), respectively. The calculated stabilization energy of the complexes investigated has been corrected from the basis set superposition error (BSSE) by the full counterpoise technique.[35] For the EDA CO_2 complex formed with methanol, the optimized structure and the computed interaction energy found from both MP2/aug-cc-pVDZ and MP2/cc-pVTZ calculations are presented**.** Then, we have discussed only the results obtained for the two other studied complexes at the MP2/aug-cc-pVDZ level of calculation by considering that only minor deviations have been generally found comparatively with results using the cc-pVTZ basis set. Finally, vibrational analyses were carried out within the standard Wilson FG matrix formalism[36] from the appropriate optimized structures of the complex and their corresponding individual moieties using the MP2/aug-cc-pVDZ level of calculations (the size of the Dunning cc-pVTZ basis precluded us from carrying out the vibrational analysis for the complexes investigated here at the MP2 level of the perturbation theory). In this theoretical framework, the computed frequency values are assumed to be harmonic whereas the experimental ones include generally anharmonic contributions. Finally, although an immediate comparison with experimental frequency shifts due to the formation of a complex is rather tenuous, it can be argued that the trend in the computed frequency shifts is similar to that of the experimental ones.[37,38−40]

3. EDA Systems with Donating O Atom of sp^3 Type

3-1. Study of the CO_2−CH_3OH Complex. 3-1a. Structure and Stabilization Energy of the CO_2−CH_3OH Complex. The optimized structure of the isolated CO_2−CH_3OH complex is displayed in Figure 1. The structural variables (interatomic distances, angles, and dihedral angles) are defined in Figure 1, and their optimized values for each basis sets used are listed in Table 1. The equilibrium geometry of the complex is found with CO_2 above the OH bond of methanol for which the "lone pairs" of the donating O atom interact with the accepting C atom of CO_2 (cf. Figure 1). Although no symmetry of the CO_2−CH_3OH complex has been initially imposed, the final structure after the geometry optimization procedure is found to have quasi-C_s symmetry at the MP2/aug-cc-pVDZ computational level and full C_s symmetry at the MP2/cc-pVTZ level. In this latter basis set, the $R_{(C\cdots O)}$ distance between the electron donor O atom of methanol and the electron acceptor C atom of CO_2 is about 2.734 Å with an intermolecular angle $\alpha_{H-O\cdots C}$ of 133.97° (instead of about 2.729 Å and 132.39°, respectively, using the aug-cc-pVDZ basis set) (see Table 1). We have also determined the structural parameters for the methanol monomer

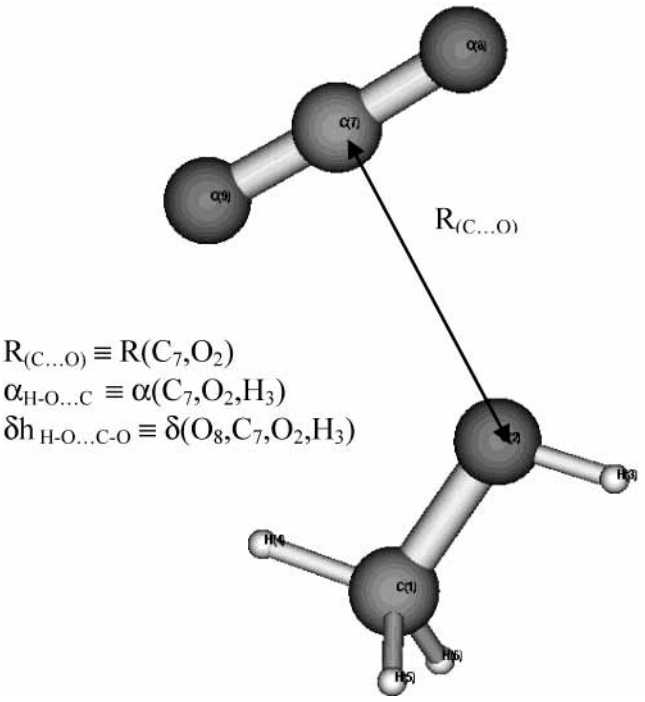

Figure 1. Schema of the optimized geometry of the CO_2−CH_3OH complex.

in its staggered conformation (C_s symmetry); these have been gathered in Table 1. These values are consistent with those reported in previous works using similar calculation levels and basis sets.[41,42] For the monomer CO_2 having $D_{\infty h}$ symmetry, the computed OC bond lengths are 1.180 and 1.169 Å using the aug-cc-pVDZ and cc-pVTZ basis sets, respectively. Clearly, the computed intramolecular distances R_{CO} and R_{HO} of methanol are slightly augmented under the complex formation, with deviation values varying from 2.5×10^{-3} to 3.1×10^{-3} Å and from 0.5×10^{-4} to 5.1×10^{-4} Å, respectively. For the CO_2 molecule, the Lewis acid−base interaction with methanol affects the internal OC bond lengths because of the repelling effect of the oxygen atoms and modifies the bond angles ∠OCO that are in the plane formed by CO_2 and the O···C intermolecular direction (cf. Table 1). These angular deviations are found to be about 2.03 and 2.23° using the aug-cc-pVDZ and cc-pVTZ basis sets, respectively. As discussed below, these structural deviations induced by the complex formation are expected to strongly affect the vibrational spectra associated with the internal modes of CO_2.

The calculated binding energy of the CO_2−CH_3OH complex $\Delta E^{(cor)}$, taking into account the BSSE energy correction $\Delta E^{(BSSE)}$, ranges from −2.972 kcal/mol at the MP2/aug-cc-pVDZ level to −2.757 kcal/mol at the MP2/cc-pVTZ level (Table 2). We have also reported in this Table the values of the electron correlation energy $\Delta E^{(MP2)}$ to evaluate their contribution to the total interaction energy. This $\Delta E^{(MP2)}$ contribution is found to be slightly lower at the MP2/cc-pVTZ level than at the MP2/aug-cc-pVDZ level whereas this trend is reversed for the contribution due to the BSSE energy correction $\Delta E^{(BSSE)}$. Finally, the electron correlation energy effects contribute about 30−35% to the total interaction energy (cf. Table 2).

3-1b. Vibrational Spectra of the CO_2−CH_3OH Complex. We have studied here the IR and Raman bands associated with the more pertinent vibrational modes that are able to probe the EDA interactions with a particular emphasis on the splitting of the ν_2 bending mode of CO_2 and the ν_S(OH) stretching mode of methanol. We have listed in Table 3 the calculated harmonic

TABLE 1: Computed Structural Parameters for the CH_3OH Monomer (C_s symmetry) and the CO_2-CH_3OH Complex at the MP2/aug-cc-pVDZ and MP2/cc-pVTZ Levels of the Perturbation Theory[a]

	optimized structure of the CH_3OH monomer	
	MP2/aug-cc-pVDZ	MP2/cc-pVTZ
$R(C_1, O_2)$	1.43489 Å	1.41848 Å
$R(H_3, O_2)$	0.96575 Å	0.95946 Å
$R(H_4, C_1)$	1.09743 Å	1.085535 Å
$R(H_{\{5,6\}}, C_1)$	1.10302 Å	1.09135 Å
$\alpha(H_3,O_2, C_1)$	107.897	107.430
$\alpha(H_4, C_1, O_2)$	106.299	106.785
$\alpha(H_{\{5,6\}}, C_1, O_2)$	111.873	112.347
$\delta(H_4, C_1, O_2, H_3)$	180.	180.
$\delta(H_{\{5,6\}}, C_1, O_2, H_3)$	±61.485	±61.516
	optimized structure of the CO_2-CH_3OH complex[b]	
$R(C_1, O_2)$	1.43740 Å	1.42109 Å
$R(H_3, O_2)$	0.96580 Å	0.95964 Å
$R(H_4, C_1)$	1.09708 Å	1.08519 Å
$R(H_5, C_1)$	1.10242 Å	1.09064 Å
$R(H_6, C_1)$	1.10242 Å	1.09064 Å
$R(C_7, O_2)$	2.73416 Å	2.72969 Å
$R(O_8, C_7)$	1.17918 Å	1.16857 Å
$R(O_9, C_7)$	1.18064 Å	1.16976 Å
$\alpha(H_3, O_2, C_1)$	108.327	108.103
$\alpha(H_4, C_1, O_2)$	106.066	106.465
$\alpha(H_5, C_1, O_2)$	111.644	112.061
$\alpha(H_6, C_1, O_2)$	111.644	112.061
$\alpha(C_7, O_2, H_3)$	133.972	132.394
$\alpha(O_8, C_7, O_2)$	94.341	93.6951
$\alpha(O_9, C_7, O_2)$	87.638	88.535
$\delta(H_4, C_1, O_2, H_3)$	−179.999	180.
$\delta(H_5, C_1, O_2, H_3)$	−61.416	−61.478
$\delta(H_6, C_1, O_2, H_3)$	+61.418	+61.478
$\delta(C_7, O_2, H_3, C_1)$	179.906	180.
$\delta(O_8, C_7, O_2, C_1)$	179.929	180.
$\delta(O_9, C_7, O_2, C_1)$	−0.071	0.

[a] The distances are given in angstroms, and the angles and dihedral angles, in degrees. Geometry optimization was carried out without the symmetry constraint even if the final configuration of the complex is found with C_s symmetry at the MP2/aug-cc-pVTZ level. [b] Notice that the structural variables of the CO_2-CH_3OH complex are defined in Figure 1.

TABLE 2: Computed Interaction Energies Corrected from the BSSE Contribution of the CO_2-CH_3OH Complex in the Optimized Geometry at the MP2/aug-cc-pVDZ and MP2/aug-cc-pVTZ Levels of the Perturbation Theory[a]

basis sets	$\Delta E_{int}^{(cor)}$[b]	$\Delta E_{int}^{(BSSE)}$	$\Delta E_{int}^{(MP2)}$[c]	$\Delta E_{int}^{(cor-ZPE)}$[d]
cc-pVTZ	−2.757	+1.015	−0.800	n.c.
aug-cc-pVDZ	−2.972	+0.878	−1.049	−2.337

[a] The energy values are given in kcal/mol. [b] $\Delta E_{int}^{(cor)}$ interaction energy calculated at the MP2 level corrected from the BSSE contribution $\Delta E_{int}^{(BSSE)}$. [c] $\Delta E_{int}^{(MP2)} = \Delta E_{int}^{(cor)} - [\Delta E_{int}^{(cor)}]_{RHF}$, where $[\Delta E_{int}^{(cor)}]_{RHF}$ is the RHF energy contribution of the complex. [d] $\Delta E_{int}^{(cor-ZPE)} = [\Delta E_{int}^{(cor)}]_{(MP2)} + \Delta ZPE$ ($CH_3OH{\cdot}CO_2$), where $\Delta E_{int}^{(cor-ZPE)}$ is the zero-point energy correction to the total binding energy of the isolated $CH_3OH{\cdot}CO_2$ dimer.

frequencies, the infrared intensities, and the Raman activities with their corresponding depolarization ratio ρ associated with each vibrational mode of the complex and for each isolated species using the MP2/aug-cc-pVDZ computational level. The comparison of the two sets of data obtained for each internal mode enables us to deduce the frequency shifts and the intensity variations (IR and Raman) due to the complex formation. The five lowest-frequency modes (with wavenumbers less than 160 cm^{-1}) are assigned to the external (intermolecular) modes whereas the modes situated at frequency values greater than 300 cm^{-1} correspond to the perturbed internal vibrations of the two interacting moieties. For the sake of convenience, we have also displayed in Figure 2A and B, respectively, the predicted infrared and Raman spectra.

In infrared absorption, the two vibrationally active modes of isolated CO_2 are the ν_2 bending mode (doubly degenerate) and the antisymmetric ν_3 stretching mode, which is the most intense. In Raman spectroscopy, only the symmetric ν_1 stretching mode of CO_2 is active (cf. Figure 2A and B). Upon CO_2-CH_3OH complex formation, the degeneracy of the ν_2 bending mode is removed, leading to a frequency splitting $\Delta\nu_2$ with a value of 16.4 cm^{-1}. It is noteworthy that the value of the splitting $\Delta\nu_2$ reported in the literature from calculations at the SCF/3-21G* level was evaluated at about 23.7 cm^{-1}.[3] Comparison with observed IR spectra for a series of compounds interacting with CO_2 (DMSO, acetone, etc.)[4] has shown that the values of $\Delta\nu_2$ were always overestimated by a factor approximately of 2. Clearly, our results indicate that by taking into account the electron correlation contribution the value of the splitting of the ν_2 mode is lowered. We assign the $\nu_2^{(1)}$ mode situated at the lowest frequency to the perturbed OCO bending motion of CO_2 in the plane formed by CO_2 and the O···C intermolecular bond (see Figure 1). The IR intensity of the $\nu_2^{(1)}$ mode is enhanced by a factor of 1.95 compared with its intensity for the "free" CO_2 (Table 3). Moreover, the $\nu_2^{(1)}$ mode shifts toward lower wavenumbers by values of $\Delta\nu_2^{(1)} = 14.4$ cm^{-1}. The $\nu_2^{(2)}$ mode situated at higher frequency is assigned to the OCO bending mode of CO_2 out of the plane formed by CO_2 and the O···C intermolecular bond. The IR intensity associated with this mode is slightly reduced by a factor of 0.9 compared with that of the bending mode of the free CO_2. The $\nu_2^{(2)}$ mode is shifted toward higher frequencies by a value of 2.0 cm^{-1} compared with that of the free CO_2. In Raman spectroscopy, the ν_2 mode, which is inactive for the free CO_2, leads to the apparition of a doublet upon complex formation. The intensity of the low-frequency $\nu_2^{(1)}$ mode is greater than that of the $\nu_2^{(2)}$ mode by a factor of 45.0. Incidentally, we found from the values of the depolarization ratios that the $\nu_2^{(1)}$ mode is polarized whereas the $\nu_2^{(2)}$ mode is depolarized (cf. Table 3).

If we consider now the ν_1 symmetric stretching mode of free CO_2, which is inactive in infrared spectroscopy and strongly active in Raman scattering, we note that this mode is not drastically affected upon complex formation. Indeed, this mode is only slightly shifted to higher frequencies by 3.2 cm^{-1}. Its Raman intensity decreases by a factor of 0.93. Though the ν_1 mode becomes active in the complex, the computed IR intensity is very small, with a value lower at least by several orders of magnitude than the authorized modes of CO_2.

Similar conclusions are reached for the ν_3 stretching mode of CO_2. Indeed, in IR, this mode is also weakly shifted toward higher wavenumbers by 2.7 cm^{-1}, and its intensity is reduced by a factor of about 0.94 compared with that of the free CO_2. In Raman, this mode becomes active with complex formation, but again, its intensity is still much lower than those of the authorized modes (cf. Table 3). Now, we consider the perturbation of the internal modes of the CH_3OH moiety under complex formation. Two normal modes of vibration are particularly affected. The former is the ν(CO) stretching mode of methanol (labeled 10(A″) in Table 3), which is shifted toward higher wavenumbers by about 1.7 cm^{-1}. The IR intensity is enhanced by a factor of about 1.5 whereas the Raman intensity is quasi-unaffected under complex formation. Finally, the analysis of the ν_S(OH) stretching mode of CH_3OH (labeled 20(A′) in Table 3) interacting with CO_2 is shifted toward lower wavenumbers by about 2.4 cm^{-1}. The IR intensity is enhanced by a factor of 1.14 whereas the Raman activity is slightly weakened.

TABLE 3: Calculated (Harmonic) Vibrational Frequencies (cm^{-1}), IR Intensities I_{IR} (km/mol), Raman Scattering Activities ($Å^4$/amu), and Depolarization Ratio ρ of the CH_3OH Monomer and the CH_3OH-CO_2 Complex at the MP2/aug-cc-pVDZ Level of the Perturbation Theory[a]

	CO_2 monomer			CH_3OH monomer			CO_2-CH_3OH complex		
mode labels	ν	I_{IR}	$[I_{Ram}/\rho]$	ν	I_{IR}	$[I_{Ram}/\rho]$	ν	I_{IR}	$[I_{Ram}/\rho]$
Low-Frequency Values of the External Modes of the Complex									
1							25.7	9.87	[0.07/0.75]
2							73.15	7.91	[0.09/0.75]
3							81.7	2.77	[0.94/0.75]
4							107.1	0.38	[0.30/0.70]
5							148.4	1.29	[1.47/0.73]
6-(A″)				311.1	104.93	[0.89, 0.75]	320.4	105.77	[0.77/0.75]
7-ν2(OCO) bending	655.5	21.46					641.1 657.5	41.87 19.57	0.45/0.475] [0.01/0.75]
8-(A′)				1044.1	112.30	[4.05, 0.19]	1041.9	102.43	[3.93/0.15]
9-(A′)				1074.9	0.63	[5.62, 0.20]	1072.0	2.11	[4.98/0.22]
10(A")				1169.1	0.39	[0.92, 0.75]	1170.8	0.59	[0.96/0.75]
11-ν1(OC)	1305.4		[33.38/0.14]				1308.2	.29	[31.01/0.11]
12-(A′)				1366.3	22.13	[1.29, 0.53]	1361.4	16.54	[1.14/0.65]
13-(A′)				1465.1	4.45	[0.79, 0.24]	1463.1	1.04	[0.90/0.45]
14-(A″)				1493.6	2.54	[4.84, 0.75]	1496.4	2.26	[4.28/0.75]
15-(A′)				1505.1	4.59	[5.10, 0.75]	1503.9	5.02	[5.90/0.71]
16-ν3(OC)	2379.2	567.59					2381.9	532.41	[0.36/0.75]
17-(A′)				3053.1	56.62	[164.1, 0.02]	3057.3	56.45	[164.4, 0.03]
18-(A″)				3130.6	44.73	[58.23, 0.75]	3137.7	39.07	[61.31, 0.75]
19-(A′)				3189.8	21.88	[54.92, 0.57]	3195.7	13.43	[37.17, 0.59]
20-(A′)				3841.6	34.41	[71.17, 0.16]	3839.2	39.33	[69.96, 0.15]

[a] Experimentally, the ν_2 bending and the ν_3 stretching modes are respectively situated at about 667 and 2349. cm^{-1} for CO_2 in the gas phase (P. Lalanne, Ph.D. Thesis, ref 27 and references therein). In the literature, it is clearly established that the SCF/6-31G calculations provided a very good estimation for the ν_2 bending mode of free CO_2 in comparison with the experimental value. Notice that in our calculations the calculated frequency values at the MP2/aug-cc-pVDZ level are found to be the closest to the experimental ones.

3-2. Study of the $CO_2-CH_3CH_2OH$ Complex. 3-2a. Structure and Stabilization Energy of the $CO_2-CH_3CH_2OH$ Complex. The equilibrium structure of the $CO_2-CH_3CH_2OH$ complex has been calculated as previously without symmetry constraint at the MP2/aug-cc-pVDZ computational level. The optimized geometry of the complex is displayed in Figure 3, and the computed structural variables are given in Table 4. The optimized structure of the $CO_2-CH_3CH_2OH$ complex is found to have quasi-C_s symmetry in which the CO_2 molecule is situated above the OH bond of ethanol for which the lone pairs of the donating O atom interact with the accepting C atom of CO_2. The distance $R_{(C\cdots O)}$ between the electron donor O atom of ethanol and the electron acceptor C atom of CO_2 is 2.75 Å. The ethanol molecule interacting with CO_2 is nearly in its trans conformation (C_s symmetry). For comparison, the structural parameters of the isolated *trans*-ethanol monomer (C_s symmetry) that are in good agreement with those calculated using similar level of calculation and basis set reported in the literature[43] are also gathered in Table 4. Clearly, under complex formation, the intramolecular distances R_{CO} and R_{HO} of ethanol are increased, with values ranging from 2.4×10^{-3} and 3.0×10^{-4} Å, respectively (Table 4). For the CO_2 molecule, the EDA interaction with ethanol leads to small changes in the internal OC bond length and the bond angle OCO (see Table 4), which is slightly distorted with an angular deviation of 1.89°. Finally, the calculated binding energy of the $CO_2-CH_3CH_2OH$ complex $\Delta E^{(cor)}$ corrected from the BSSE energy ($\Delta E^{(BSSE)} \approx 1.003$ kcal/mol) is found to contain an electron correlation contribution to the energy $\Delta E^{(MP2)}$ of -1.296 kcal/mol, a trend previously observed with the CO_2-CH_3OH complex. If we also take into account the zero-point energy (ZPE) correction, then the interaction energy $\Delta E^{(cor-ZPE)}$ reaches a value of -2.417 kcal/mol.

3-2b. Vibrational Spectra of the $CO_2-CH_3CH_2OH$ Complex. In Table 5, we have reported the calculated values of the frequency and the IR and Raman intensities associated with each vibrational mode for the complex and the isolated moieties CH_3CH_2OH and CO_2. The five lowest-frequency modes reported in this Table are assigned with the external modes arising under complex formation whereas beyond 200 cm^{-1} the vibrational modes correspond to the perturbed internal modes under complex formation. We have shown in Figure 4A and B the computed infrared and Raman spectra of the $CO_2-CH_3CH_2OH$ complex at the MP2/aug-cc-pVDZ level. As for the complex with methanol, the degeneracy of the ν_2 bending mode of CO_2 with ethanol is removed, and the frequency splitting $\Delta\nu_2$ is about 17.1 cm^{-1}. This value is very close to the calculated splitting of the ν_2 mode of CO_2 interacting with CH_3OH (section 3-1b) but is found to be slightly less than the value reported at the SCF/3-21G* level by Jamroz and coworkers.[3]

The lowest-frequency $\nu_2^{(1)}$ mode is assigned as the perturbed OCO bending motion of CO_2 in the plane formed by CO_2 and the O···C intermolecular direction (see Figure 3). Compared with the ν_2 mode of isolated CO_2, the $\nu_2^{(1)}$ mode has been shifted toward lower frequency by a value of $\Delta\nu_2^{(1)}$ equal to 15.1 cm^{-1}. The IR intensity associated with this $\nu_2^{(1)}$ mode is enhanced by a factor of 2.0. The highest-frequency $\nu_2^{(2)}$ mode is assigned to the weakly perturbed OCO bending motion of CO_2 out of the plane formed by CO_2 and the O···C intermolecular bond. This mode is shifted toward higher frequencies by a value of $\Delta\nu_2^{(2)}$ of 2.0 cm^{-1} compared with the ν_2 mode of free CO_2. The IR intensity is reduced by about 10%. In Raman spectroscopy, the doublet structure is observed, and the intensity of the $\nu_2^{(1)}$ mode is greater by a factor of about 37 than that of the $\nu_2^{(2)}$ mode (Table 5). As for the CO_2-CH_3OH complex (section 3-1b), the

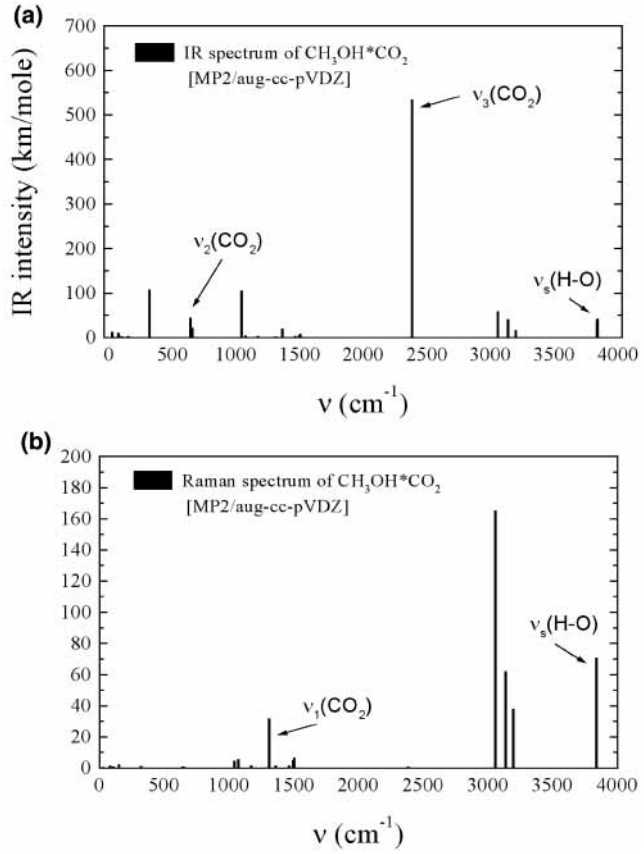

Figure 2. IR absorption lines (A) and Raman spectrum (B) of the CO_2*CH_3OH complex calculated at the MP2/aug-cc-pVDZ level.

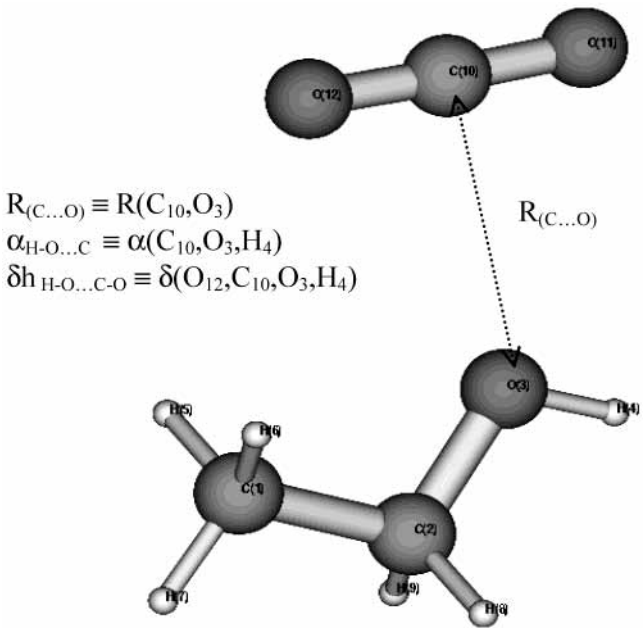

Figure 3. Schema of the optimized geometry of the CO_2−CH_3CH_2OH complex.

computed depolarization ratio shows that the $\nu_2^{(1)}$ mode is depolarized whereas the $\nu_2^{(2)}$ mode is polarized. The ν_1 mode of CO_2 is shifted toward higher frequency of about +2.9 cm^{-1}, and its IR intensity is 2 orders of magnitude less than those of the authorized modes of CO_2. The Raman intensity of this mode is decreased by a factor of 0.9. The ν_3 stretching mode of CO_2 is found to be weakly perturbed under complex formation. It is slightly shifted toward higher wavenumbers by a value of 2.7 cm^{-1}, and its IR intensity is decreased by a factor of 0.92. Finally, the ν_S(OH) mode of ethanol (labeled 29-(A′) in Table 5) interacting with CO_2 is shifted toward lower wavenumbers by a value of 5.0 cm^{-1}. The IR intensity associated with this mode is enhanced up to a value that is 15% greater than that of the corresponding mode of the ethanol monomer. In Raman, the intensity is decreased by 20%.

TABLE 4: Computed Structural Parameters for the C_2H_5OH Monomer (C_s Symmetry) and the CO_2−C_2H_5OH Complex at the MP2/aug-cc-pVDZ Level

C_2H_5OH monomer (C_s symmetry)		CO_2−C_2H_5OH complex[a]	
$R(C_1, C_2)$	1.51945 Å	$R(C_1, C_2)$	1.51932 Å
$R(C_2, O_3)$	1.44007 Å	$R(C_2, O_3)$	1.44246 Å
$R(H_4, O_3)$	0.96643 Å	$R(H_4, O_3)$	0.96672 Å
		$R(H_5, C_1)$	1.09986 Å
$R(H_{\{5,6\}}, C_1)$	1.10126 Å	$R(H_6, C_1)$	1.09986 Å
$R(H_7, C_1)$	1.10133 Å	$R(H_7, C_1)$	1.10126 Å
		$R(H_8, C_2)$	1.10459 Å
$R(H_{\{8,9\}}, C_2)$	1.10459 Å	$R(H_9, C_2)$	1.10459 Å
		$R(C_{10}, O_3)$	2.75450 Å
		$R(O_{11}, C_{10})$	1.18012 Å
		$R(O_{12}, C_{10})$	1.17969 Å
$\alpha(C_1, C_2, O_3)$	107.195	$\alpha(C_1, C_2, O_3)$	107.343
$\alpha(H_4, O_3, C_2)$	108.191	$\alpha(H_4, O_3, C_2)$	108.548
$\alpha(H_{\{5,6\}}, C_1, C_2)$	110.235	$\alpha(H_5, C_1, C_2)$	110.427
		$\alpha(H_6, C_1, C_2)$	110.427
$\alpha(H_7, C_1, C_2)$	110.265	$\alpha(H_7, C_1, C_2)$	109.982
		$\alpha(H_8, C_2, O_3)$	110.090
$\alpha(H_{\{8,9\}}, C_2, O_3)$	110.342	$\alpha(H_9, C_2, O_3)$	110.090
		$\alpha(C_{10}, O_3, H_4)$	114.702
		$\alpha(O_{11}, C_{10}, O_3)$	88.967
		$\alpha(O_{12}, C_{10}, O_3)$	92.919
$\delta(H_4, O_3, C_2, C_1)$	180.	$\delta(H_4, O_3, C_2, C_1)$	180.
$\delta(H_{\{5,6\}}, C_1, C_2, O_3)$	±59.916	$\delta(H_5, C_1, C_2, O_3)$	+59.919
		$\delta(H_6, C_1, C_2, O_3)$	−59.919
$\delta(H_7, C_1, C_2, O_3)$	180.	$\delta(H_7, C_1, C_2, O_3)$	180.
		$\delta(H_8, C_2, O_3, H_4)$	+59.662
$\delta(H_{\{8,9\}}, C_1, C_2, O_3)$	±59.762	$\delta(H_9, C_2, O_3, H_4)$	−59.662
		$\delta(C_{10}, O_3, H_4, C_2)$	180.
		$\delta(O_{11}, C_{10}, O_3, C_2)$	180.
		$\delta(O_{12}, C_{10}, O_3, H_4)$	180.

[a] No symmetry has been imposed in the geometry optimization of the CO_2−C_2H_5OH complex, though the final configuration is found to have C_s symmetry.

3-3. EDA with a Donating O Atom of sp^2 Type: CO_2−$(CH_3)_2CO$ Complex. 3-3a. Structure and Stabilization Energy of the CO_2−$(CH_3)_2CO$ Complex. The equilibrium structure of the CO_2−$(CH_3)_2CO$ complex corresponding to the lowest interaction energy is displayed in Figure 5 (structure A), and the calculated structural variables are gathered in Table 6. The binding energy $\Delta E^{(cor)}$ (corrected from the BSSE energy $\Delta E^{(BSSE)}$) is calculated to be about −2.63 kcal/mol (Table 7) and has a value that is 2 times lower than that calculated by Jamroz et al.[3] In this structure (A), the CO_2 molecule interacting with the carbonyl C═O group is situated in the molecular plane of acetone (Figure 5A). The equilibrium geometry of the CO_2−$(CH_3)_2CO$ complex is found to have quasi-C_s symmetry, as suggested by previous spectroscopic evidence.[4,12,14,15,17,26] The intermolecular distance $R_{(C\cdots O)}$ between the electron donor O atom of acetone and the electron acceptor C atom of CO_2 is 2.845 Å, and the bond length of the C═O group of acetone is increased by 1.73 10^{-3} Å compared with that of the monomer (Table 8). The EDA interaction also leads to small changes in the internal OC bond lengths of CO_2, and the bond-angle deviation of ∠OCO is 1.9°. Two other structures of the CO_2−$(CH_3)_2CO$ complex having C_{2v} symmetry have been reported. In the first structure labeled B, the C═O group (electron donor center) interacts with the C atom (electron acceptor center) of

TABLE 5: Calculated Values of (Harmonic) Vibrational Frequencies (cm^{-1}), IR Intensities I_{IR} (km/mol), Raman Scattering Activities ($Å^4$/amu), and the Depolarization Ratio ρ of the CH_3OH Monomer and the $CH_3CH_2OH-CO_2$ Complex at the MP2/aug-cc-pVDZ Level of the Perturbation Theory

	CO_2 monomer			CH_3CH_2OH monomer			$CO_2-CH_3CH_2OH$ complex		
mode labels	ν	I_{IR}	$[I_{Ram}/\rho]$	ν	I_{IR}	$[I_{Ram}/\rho]$	ν	I_{IR}	$[I_{Ram}/\rho]$
Low-Frequency Values of the External Modes of the Complex									
1							20.9	3.88	[0.27/0.75]
2							37.5	1.84	[0.33/0.75]
3							60.7	0.535	[0.50/0.75]
4							104.6	0.365	[0.39/0.69]
5							122.2	0.15	[1.84/0.74]
6-(A″)				244.7	30.82	[30.82/0.75]	253.0	15.4	[0.03/0.75]
7-(A″)				304.4	83.35	[1.09/0.75]	327.9	91.69	[0.95/0.75]
8-(A′)				411.8	10.71	[0.30/0.56]	417.4	7.18	[0.48/0.66]
9-ν2(OCO) bending	655.5	21.46					640.4 657.5	42.83 19.525	[0.37/0.52] [0.01/0.75]
10-(A")				815.8	0.06	[0.16/ 0.75]	814.6	0.04	[0.17/0.75]
11-(A′)				901.9	17.78	[6.44/ 0.15]	900.8	17.16	[5.92/0.12]
12-(A′)				1055.1	39.54	[6.61/0.12]	1055.4	31.63	[5.74/0.11]
13-(A′)				1098.6	42.01	[6.01/0.46]	1095.9	46.08	[5.64/0.46]
14-(A″)				1174.2	2.41	[0.375/0.75]	1174.3	3.050	[0.39/0.75]
15-(A′)				1269.2	57.95	[0.97/0.75]	1267.4	55.61	[1.02/0.73]
16-(A″)				1294.9	0.02	[3.49/0.75]	1294.8	0.003	[3.31/0.75]
17-ν1(OC)	1305.4		[33.38/0.14]				1308.3	0.46	[30.29/0.11]
18-(A′)				1382.5	0.91	[0.01/0.53]	1384.6	1.19	[0.09/0.72]
19-(A′)				1443.3	13.21	[2.21/0.41]	1442.5	14.53	[2.03/0.36]
20-(A")				1474.2	5.54	[4.52/0.75]	1475.5	6.785	[4.41/0.75]
21-(A′)				1492.4	2.24	[5.72/0.75]	1488.2	5.07	[6.09/0.75]
22-(A′)				1519.6	1.03	[2.68/0.75]	1518.7	0.545	[2.71/0.74]
23-ν3(OC)	2379.2	567.59					2381.9	523.46	[0.28/0.74]
24-(A′)				3043.2	60.65	[122.3/0.07]	3047.7	62.19	[122.8/0.08]
25-(A′)				3073.7	13.85	[182./0.004]	3075.2	11.12	[184.5/0.01]
26-(A")				3091.8	38.25	[85.62/0.75]	3097.8	34.40	[85.61/0.75]
27-(A")				3169.0	22.01	[50.52/0.75]	3169.5	23.65	[50.30/0.74]
28-(A′)				3176.1	25.06	[35.34/0.75]	3178.5	22.24	[28.00/0.75]
29-(A′)				3831.3	31.93	[100.1/0.19]	3826.3	37.07	[80.51/0.16]

the CO_2 molecule oriented perpendicularly to the molecular plane of acetone and forming a linear C═O···C intermolecular distance of about 2.78 Å (Table 6). The computed interaction energy $\Delta E^{(cor)}$ of the complex in this structure (B), is found to have a value of −2.352 kcal/mol including an electron correlation energy contribution of −0.617 kcal/mol (Table 7). Upon complex formation, the bond length of the C═O group varies only by about 4.8×10^{-4} Å. Small variations in the bond lengths of CO_2 are found, and the angle deviation of ∠OCO is about 1.6°. In the second structure (C), the C═O electron donor group also forms a linear C═O···C interaction with the electron acceptor C atom with a distance of about 2.87 Å. However, the molecular axis of CO_2 is perpendicularly oriented to the C═O bond but this time is contained in the molecular plane of acetone (see Figure 5 and computed values in Table 6). The computed interaction energy $\Delta E^{(cor)}$ of the complex in this conformation is found with a binding energy of −1.94 kcal/mol (Table 7). Finally, the DAE $CO_2-(CH_3)_2CO$ interaction favors the formation of a complex with quasi-C_s symmetry (Figure 5A) rather than those having C_{2v} symmetry. This trend is consistent with previous findings carried out at a lower computational level (SCF/3-21G*),[1,3] although in our study the binding energies are significantly lower, taking into account the electron correlation effects.

3-3b. Vibrational Spectra of the $CO_2-(CH_3)_2CO$ Complex. The values of the computed frequencies and the IR and Raman intensities associated with the internal modes of CO_2 and the CCC and CO stretches of $(CH_3)_2CO$ in structures A, B, and C of the complex are gathered in Table 9 and can be compared with those obtained for the acetone molecule (Table 6).

In the equilibrium structure A, the degeneracy of the ν_2 bending mode of CO_2 is removed, leading to a frequency splitting $\Delta\nu_2$ of about 18.0 cm^{-1}, a value greater than that at the computational SCF/3-21G* level (∼12.6 cm^{-1}).[3] The $\nu_2^{(1)}$ mode assigned to the OCO bending motion in the plane formed by CO_2 and the molecular plane of acetone (see Figure 5A) is shifted toward lower wavenumbers by 15.9 cm^{-1}, and its IR intensity is enhanced by a factor of 2.1. The highest-frequency mode $\nu_2^{(2)}$ attributed to the OCO bending mode of CO_2 out of the plane is slightly shifted toward higher frequencies by 2.1 cm^{-1} whereas its IR intensity is decreased by 10%. In Raman spectroscopy, the intensity of the $\nu_2^{(1)}$ mode of the doublet is found to be 2 orders of magnitude greater than that of the $\nu_2^{(2)}$ mode.

In structures B and C of the complex, the values of the splitting of the ν_2 mode of CO_2 are respectively 11.4 and 10.4 cm^{-1}, which are found to be smaller than the computed value (∼18 cm^{-1}) in structure A (Table 9). The shift toward the lower wavenumbers of the $\nu_2^{(1)}$ mode predicted for structures B and C is 9.5 cm^{-1}, a value smaller than for structure A according to a smaller value of the angle deviation of ∠OCO in CO_2. The IR intensity of the $\nu_2^{(1)}$ mode is enhanced by factors of 2.1 (structure B) and 1.9 (structure C). The IR intensity associated with the $\nu_2^{(2)}$ mode is diminished by about 10%, a value comparable to the one obtained for structure A.

Under the formation of the $CO_2-(CH_3)_2CO$ complex, the ν_1 mode of CO_2 is found to be slightly shifted toward higher

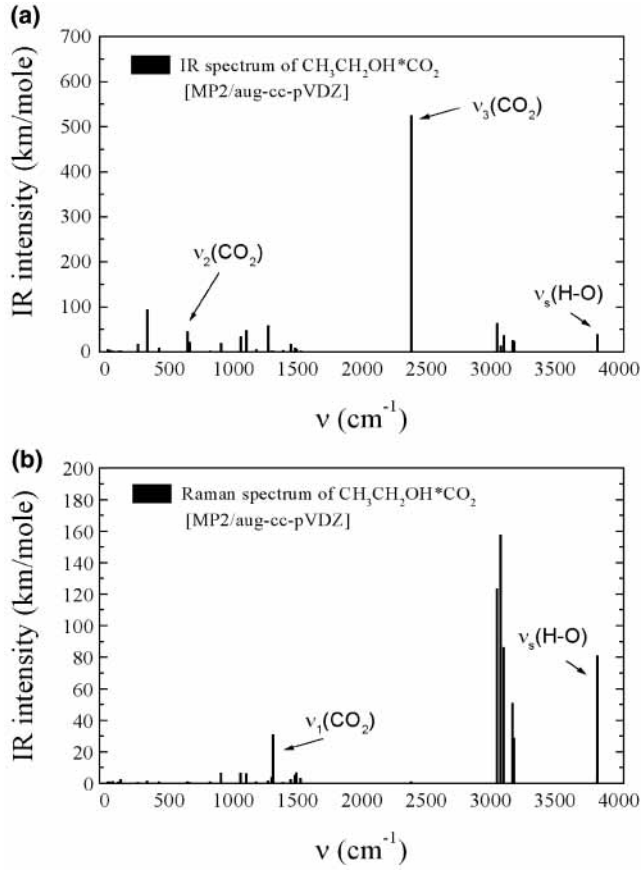

Figure 4. IR absorption lines (A) and Raman spectrum (B) of the CO_2*CH_3CH_2OH complex calculated at the MP2/aug-cc-pVDZ level.

frequency by values of 2.7 cm^{-1} (structure A), 3.5 cm^{-1} (structure B), and 3.1 cm^{-1} (structure C). The IR intensity of the ν_1 mode is lower by 2 orders of magnitude compared with those of the authorized modes of free CO_2. The Raman intensity of this mode is decreased by a factor ranging from 0.96 (structure A) to 0.91 (structure C).

The ν_3 stretching mode of the inner CO_2 for the three structures of the complex is weakly perturbed, as indicated by shifts toward the higher wavenumbers with values ranging from 2.3 cm^{-1} (structure A) to 3.8 cm^{-1} (structure B). Moreover, its IR intensity is slightly diminished by a factor about 0.9. The antisymmetric ν_a(CCC) stretching mode of acetone interacting with CO_2 is shifted toward greater frequency values of about 3.1 cm^{-1} (structure A), 1.3 cm^{-1} (structure B), and 1.6 cm^{-1} (structure C). The IR intensity associated with this mode is weakly decreased in structures A and B whereas it is slightly enhanced by 1.07 for structure C. The Raman activity is increased by a factor ranging from 1.5 to 1.8 in the structure B.

Finally, the spectral signature providing information about the structure of the complex can be assessed from the symmetric ν_S(CO) stretching mode of acetone. Indeed, in the equilibrium structure (A), this mode is shifted by 2.2 cm^{-1} toward lower frequency whereas, in contrast, in structures B and C the shifts are found toward higher wavenumbers, with a common value of about 3.4 cm^{-1} (Table 9). Moreover, the IR intensities of this mode are found to be enhanced by a factor ranging from 1.13 in structure A to 1.2 for structures B and C. Furthermore, the Raman activity is not affected by the complex formation whereas it is increased to 1.4 in structures A and B compared with that of free acetone.

4. Discussion and Conclusions

The discussion of the results presented so far can be carried out from a comparison with literature ab initio results. Here, this issue concerns the choice of the basis set used and also the influence of the electron correlation effects on both the structural and vibrational spectroscopic features of the EDA CO_2 complexes belonging to the class of sp^3 donating O atoms (methanol and ethanol) and the sp^2 donating O atom of acetone.

4-1. Predicted Structural Properties of EDA Complexes. As a preliminary conclusion, the predicted structures for all of these EDA complexes are found to be rather similar, independent of the size of the basis sets and the computational level used (including electron correlation or not) compared with the calculations at the SCF/3-21G* level reported in ref 3. Nevertheless, the stabilization energies are found in our work to be 2 to 2.5 times lower including electron correlation. The lack of knowledge of the experimental binding energies of these EDA CO_2 complexes precludes us from settling the choice of a particular method of calculation. However, the predictions are in qualitative agreement with the structures of the complexes deduced from IR experimental evidence for CO_2 dissolved in liquid alcohols[4] and for CO_2 with a carbonyl group.[4,12,26]

4-2. Characteristic Vibrational Features of EDA Complexes. 4-2a. CO_2 Moiety. For all the EDA complexes investigated, it is found that the splitting of the ν_2 mode of CO_2 is strongly correlated with the arrangement of inner CO_2. The strongest perturbation is always experienced by the bending motion in the plane formed by CO_2 and the O···C intermolecular bond. This involves a significant shift of mode $\nu_2^{(1)}$ toward lower wavenumbers, accompanied by a strong enhancement of its IR intensity, which is 2 times lower than that of the ν_2 mode of free CO_2. Moreover, the out-of-plane bending mode $\nu_2^{(2)}$ of CO_2 is shifted toward higher wavenumbers, and its intensity is barely lowered compared with that of free CO_2. However, in contrast to a previous study carried out at the SCF computational level,[1,3] we found that there is no convincing general relationship between the splitting of the ν_2 mode of CO_2 and the stabilization energy by taking into account the electron correlation contribution for EDA CO_2 complexes formed with sp^3 donors (methanol and ethanol) or an sp^2 donor (acetone). However, for a given class, namely, sp^2 donor CO_2 complexes with acetone, our spectral analyses of the different structures do confirm that the splitting of the ν_2 mode of CO_2 increases with the stability of the complex. Our vibrational analysis confirms that the symmetric ν_1 and antisymmetric ν_3 stretches of CO_2 are weakly perturbed (shifts, IR and Raman intensities) by the EDA complex formation for both sp^3 donor and sp^2 donor classes.

4-2b. Donor Moieties. For the sp^3 donor class, our findings clearly indicate that the ν_S(OH) stretching mode of alcohols interacting with CO_2 appears to be (not surprisingly) the best-adapted vibration to probe the complex formation. Indeed, this ν_S(OH) mode is shifted toward lower frequencies, and its IR intensity is significantly enhanced. We postpone our discussion to the next section to compare our results with IR experimental observations.

For the sp^2 donor CO_2 complex, we clearly show that the ν_a(CCC) and ν_S(CO) stretching vibrations exhibit spectral features that are well adapted to the investigation of EDA complex formation. The ν_a(CCC) stretch of acetone is shifted toward higher frequencies, and its IR intensity is moderately decreased in comparison with the isolated acetone whereas the Raman activity is significantly enhanced. The ν_S(CO) stretch of the C═O group is shifted toward the lower frequencies for the complex in the structure A. The IR intensity of this mode

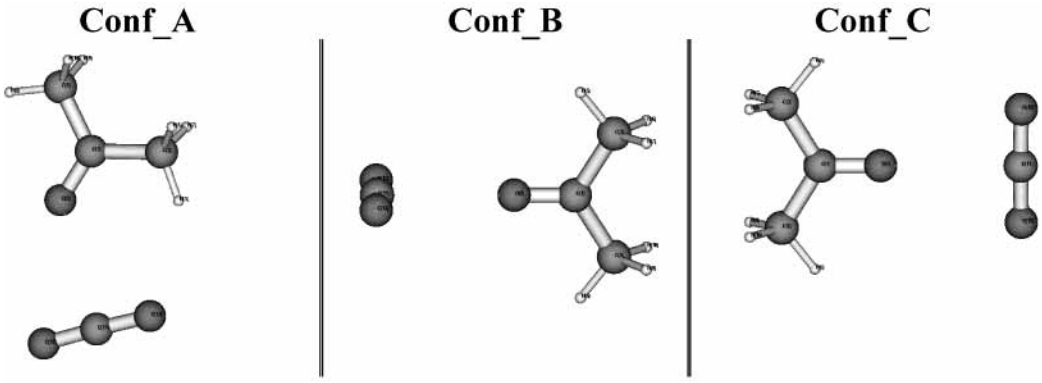

Figure 5. Structures of the $CO_2-(CH_3)_2CO$ complex calculated at the MP2/aug-cc-pVDZ level.

TABLE 6: Structural Parameters of the $CO_2-(CH_3)_2CO$ Complex for Structures [A], [B], and [C] Computed at the MP2/aug-cc-pVDZ Level

	$CO_2-(CH_3)_2CO$ Complex		
	conf. [A]	conf. [B]	conf. [C]
Distances		Distances	
$R(C_1, O_2)$	1.23248 Å	$R(C_1, O_2)$	1.23123 Å	1.23106 Å
$R(C_1, C_3)$	1.51646 Å	$R(C_1, C_{\{3,4\}})$	1.51657 Å	1.51689 Å
$R(C_1, C_4)$	1.51669 Å	$R(C_3, H_5) = R(C_4, H_8)$ $R(C_4, H_8)$	1.09726 Å	1.09730 Å
$R(C_3, H_5)$	1.09667 Å	$R(C_3, H_{\{6,7\}}) = R(C_4, H_{\{9,10\}})$	1.10254 Å	1.10257 Å
$R(C_4, H_8)$	1.09715 Å	$R(O_2, C_{11})$	2.77816 Å	2.86946 Å
$R(C_3, H_{\{6,7\}})$	1.10258 Å	$R(O_{12}, C_{11}) = R(O_{13}, C_{11})$	1.17979 Å	1.17984 Å
$R(C_4, H_{\{9,10\}})$	1.10253 Å	Angles		
$R(O_2, C_{11})$	2.84556 Å	$\alpha(C_{\{3,4\}}, C_1, O_2)$	121.615	121.600
$R(O_{12}, C_{11})$	1.17821 Å	$\alpha(H_5, C_3, C_1) = \alpha(H_8, C_4, C_1)$	110.072	110.030
$R(O_{13}, C_{11})$	1.18159 Å	$\alpha(H_{\{6,7\}}, C_3, C_1) = \alpha(H_{\{9,10\}}, C_4, C_1)$	109.831	109.840
Angles		$\alpha(O_{\{12,13\}}, C_{11}, O_2)$	90.780	90.758
$\alpha(C_3, C_1, O_2)$	121.807	Dihedral Angles		
$\alpha(C_4, C_1, O_2)$	121.405	$\delta(H_{\{6,9\}}, C_3, C_1, O_2)$	+58.790	+58.773
$\alpha(H_5, C_3, C_1)$	110.188	$\delta(H\{_{7,10}\}, C_3, C_1, O_2)$	−58.790	−58.773
$\alpha(H_8, C_4, C_1)$	110.092	$\delta(H_5, C_3, C_1, C_{11}) = \delta(H_8, C_4, C_1, C_{11})$	0.	0.
$\alpha(H_6, C_3, C_1)$	109.715	$\delta(O_{12}, C_{11}, C_1, C_3) = \delta(O_{13}, C_{11}, C_1, C_4)$	90.	0.
$\alpha(H_7, C_3, C_1)$	109.715			
$\alpha(H_9, C_4, C_1)$	109.810			
$\alpha(H_{10}, C_4, C_1)$	109.810			
$\alpha(C_{11}, O_2, C_1)$	131.520			
$\alpha(O_{12}, C_{11}, O_2)$	89.464			
$\alpha(O_{13}, C_{11}, O_2)$	92.423			
Dihedral				
$\delta(H_6, C_3, C_1, O_2)$	+58.664			
$\delta(H_{10}, C_3, C_1, O_2)$	−58.742			
$\delta(H_7, C_3, C_1, O_2)$	−58.654			
$\delta(H_9, C_3, C_1, O_2)$	+58.751			
$\delta(H_5, C_3, C_1, O_2)$	0.005			
$\delta(H_8, C_4, C_1, O_2)$	0.004			
$\delta(C_{11}, O_2, C_1, C_3)$	−0.009			
$\delta(O_{12}, C_{11}, O_2, C_1)$	−179.996			
$\delta(O_{13}, C_{11}, O_2, C_1)$	+0.004			

TABLE 7: Computed Interaction Energies, Corrected from the BSSE Contribution, at the MP2/aug-cc-pVDZ Level of the $CO_2-(CH_3)_2CO$ Complex in Structures [A], [B], and [C][a]

structures	$\Delta E_{int}^{(cor)}$	$\Delta E_{int}^{(BSSE)}$	$\Delta E_{int}^{(MP2)}$	$\Delta E_{int}^{(cor-ZPE)}$
conf_A	−2.632	+1.079	+0.105	−2.078
conf_B	−2.352	+0.776	−0.617	−2.008
conf_C	−1.941	+0.708	−0.380	−1.657

[a] All energy values are given in kcal/mol.

is slightly enhanced, and the Raman activity remains unchanged in comparison with that of free acetone. In contrast, for the two other structures (B and C), the ν_S(CO) mode is predicted to shift this time toward higher frequencies, and both the IR and Raman intensities are found to increase.

4-2c. Comparison with Experimental Spectra. Our ab initio predictions can be compared with available IR and Raman measurements. However, the few experimental investigations that have been reported have been carried out only for IR absorption of the ν_2 and ν_3 modes of the acceptor (CO_2).[4,12] The main observations concern the splitting of the ν_2 mode of CO_2 in liquid acetone found to be about 5 cm^{-1}. For CO_2 dissolved in liquid methanol and ethanol, the splitting is not observed, although this mode is found to be shifted toward lower frequencies by 10 and 12 cm^{-1}, respectively.[4] In comparison with previous computed shifts at the SCF/3-21G* level,[3] our predicted values including the electron correlation are found to be closest to the experimental ones. The ν_3 mode of CO_2 has been experimentally found to be shifted toward lower frequencies in liquid solvents with values of 7. cm^{-1} (methanol), 9 cm^{-1} (ethanol), and 7 cm^{-1} (acetone), respectively. Comparison with our results shows that the trend is correct and that the calculated values (2.5 cm^{-1} for methanol, 5 cm^{-1} for ethanol, and 2.3 cm^{-1} for acetone) are in fair agreement with experimental ones.[4] For the donor molecule, we have measured the IR absorption profiles

TABLE 8: Structural Parameters and Vibrational Analysis Calculated for the Equilibrium Geometry (C_{2v} Symmetry) of the $(CH_3)_2CO$ Monomer at the MP2/aug-cc-pVDZ Level

$(CH_3)_2CO$ monomer		modes	vibrational analysis[a]		
Distances					
$R(C_1, O_2)$	1.23075 Å	1	22.2	0.	[0.16/0.75]
$R(C_1, C_{\{3,4\}})$	1.518115 Å	2	146.0	0.13	[0.007/0.75]
$R(C_3, H_5) = R(C_4, H_8)$	1.09733 Å	3	376.6	1.27	[0.62/0.72]
$R(C_3, H_{\{6,7\}}) = R(C_4, H_{\{9,10\}})$	1.10262 Å	4	479.8	0.55	[0.34/0.75]
Angles		5	526.9	14.8	[1.29/0.75]
$\alpha(C_3, C_1, O_2) = \alpha(C_4, C_1, O_2)$	121.712	6	807.0	1.36	[17.65/0.09]
$\alpha(H_5, C_3, C_1) = \alpha(H_8, C_4, C_1)$	110.008	7	873.1	0	[0.24/0.75]
$\alpha(H_{\{6,7\}}, C_3, C_1) = \alpha(H_{\{9,10\}}, C_4, C_1)$	109.891	8	893.5	4.19	[1.39/0.75]
Dihedral Angles		9	1071.5	0.02	[2.18/0.15]
$\delta(H_6, , C_3, C_1, O_2) = \delta(H_{10}, C_4, C_1, O_2)$	+58.8169	10-ν_a(CCC)	1097.3	1.15	[0.14/0.75]
$\delta(H_7, C_3, C_1, O_2) = \delta(H_9, C_4, C_1, O_2)$	−58.8169	11	1247.8	42.74	[4.40/0.75]
$\delta(H_5, C_3, C_1, O_2) = \delta(H_8, C_4, C_1, O_2)$	0.	12	1368.6	12.61	[0.81/0.69]
		13	1384.9	70.59	[0.12/0.75]
		14	1448.8	0.08	[0.675/0.75]
		15	1454.3	0	[8.60/0.75]
		16	1457.4	28.9	[13.70/0.60]
		17	1480.4	18.36	[0.01/0.75]
		18-ν_S(O═C)	1732.6	125.66	[14.31/0.57]
		19	3061.1	1.49	[0.75/0.75]
		20	3065.5	7.14	[316.5/3. × 10^{-3}]
		21	3144.3	0	[9.20/0.75]
		22	3150.2	14.91	[88.15/0.75]
		23	3198.1	9.81	[46.04/0.75]
		24	3198.9	4.64	[58.79/0.615]

[a] Calculated values of (harmonic) vibrational frequencies (cm^{-1}), IR intensities I_{IR} (km/mol), Raman scattering activities ($Å^4$/amu), and the depolarization ratio ρ

TABLE 9: Vibrational Spectral Variations under CO_2−$(CH_3)_2CO$ Complex Formation at the MP2/aug-cc-pVDZ Level for the Different Structures

frequency shifts (cm^{-1})	10^3 k (dyn $Å^{-1}$)	(k/k^0)	$(I/I^0)_{IR}$	$(I/I^0)_{Ram}$	internal modes assignments
		CO_2−$(CH_3)_2CO$ Complex in Structure A			
$\Delta\nu_2$ (1) ≈ −15.90	3.11	0.95	2.14		splitting of the ν_2
$\Delta\nu_2$ (2) ≈ +2.10	3.28	1.01	0.89		bending OCO of CO_2
+2.70	16.11	1.00		0.96	ν_1 stretching of CO_2
+2.30	42.99	1.00	0.92		ν_3 stretching of CO_2
+3.10	1.40	1.01	0.94	1.50	ν_a CCC stretching
−2.20	15.45	0.97	1.13	1.01	ν_s C═O stretching
		CO_2−$(CH_3)_2CO$ Complex in Structure B			
$\Delta\nu_2$ (1) ≈ −9.60	3.16	0.97	2.11		splitting of the ν_2
$\Delta\nu_2$ (2) ≈ +1.75	3.28	1.00	0.86		bending OCO of CO_2
+3.50	16.14	1.01		0.94	ν_1 stretching of CO_2
+3.80	43.07	1.00	0.93		ν_3 stretching of CO_2
+1.30	1.40	1.01	0.98	1.79	ν_a CCC stretching
+3.40	15.97	1.01	1.19	1.48	ν_s C═O stretching
		CO_2−$(CH_3)_2CO$ Complex in Structure C			
$\Delta\nu_2$ (1) ≈ −9.55	3.17	0.97	1.92		splitting of the ν_2
$\Delta\nu_2$ (2) ≈ +0.80	3.28	1.01	0.91		bending OCO of CO_2
+3.1	16.13	1.00		0.91	ν_1 stretching of CO_2
+3.1	43.05	1.00	0.90		ν_3 stretching of CO_2
+1.60	1.40	1.01	1.07	1.50	ν_a CCC stretching
+3.40	15.98	1.01	1.21	1.42	ν_s C═O stretching

of the ν_{OD} (∼2713 cm^{-1}) mode of deuterated ethanol and the ν_{CCC} (∼1218 cm^{-1}) and ν_{CO} (∼1730 cm^{-1}) stretches of acetone in SC CO_2 (313 K) for density values ranging from 0.03 to 0.82 g cm^{-3}.[27,44] For the ν_{OD} mode, we found that the band center is shifted toward lower wavenumbers of about 17 cm^{-1} at the highest densities investigated and that the integrated intensity is enhanced by about 25%. These trends are consistent with our ab initio predictions supporting the existence of EDA complex formation between ethanol (sp^3 donor) and CO_2.

For acetone in SC CO_2, the ν_{CCC} band center is shifted toward higher wavenumbers by about 5. cm^{-1} whereas the integrated intensity is decreased by about 30%. In contrast, the ν_{CO} mode of acetone is found shifted toward lower wavenumbers by about 10 cm^{-1}, and its intensity is increased by about 20%. These spectral features are consistent with our ab initio findings and lend support to the existence of EDA complex formation between acetone (sp^2 donor) and CO_2 which rather corresponds with the structure A. Indeed, the computed shifts of the ν_{CO} mode of acetone associated with structures B and C do not agree with experimental findings.

Finally, we emphasize the usefulness of ab initio calculations in providing insight into the vibrational spectra of EDA CO_2 complexes even if the frequency calculations are performed using the harmonic approximation. Moreover, our results show that this conclusion remains valid even if solvent environment effects are present, as for a solute diluted in SC CO_2. As a final comment, we point out that more experimental measurements, especially using Raman spectroscopy, which is still largely

unemployed in the context of investigations of EDA CO_2 complexes, are very welcome in validating the theoretical predictions discussed in this paper.

Acknowledgment. We gratefully acknowledge the support provided by the IDRIS computer center of the CNRS (Institut du Développement et des Ressources en Informatique Scientifique, Orsay) and the MASTER of the ENSPCB (Université de Bordeaux I, Talence) for allocating computing time and providing facilities. The support of the University Bordeaux I (Programs pluri-formation no. 971022 et 990814) is also gratefully acknowledged.

References and Notes

(1) Nelson, M. R.; Borkman, R. F. *J. Phys. Chem. A* **1998**, *102*, 7860.
(2) Kauffman, J. *J. Phys. Chem. A* **2001**, *105*, 3433.
(3) Jamroz, M. H.; Dobrowolski, J. C.; Bajdor, K.; Borowiak, M. A. *J. Mol. Struct.* **1995**, *349*, 9.
(4) Dobrowolski, J. C.; Jamroz, M. H. *J. Mol. Struct.* **1992**, *275*, 211.
(5) Cox, A. J.; Ford, T. A.; Glasser, L. *J. Mol. Struct.* **1994**, *312*, 101.
(6) Ford, T. A. Ab Initio Predictions of the Vibrational Spectra of Some Molecular Complexes: Comparison with Experiment. In *Molecular Interactions: From van der Waals to Strongly Bound Complexes*; Schneider, S., Ed.; John Wiley & Sons Ltd.: Chichester, U.K., 1997; p 181.
(7) Sadlej, J.; Makarewicz, J.; Chalasinski, G. *J. Chem. Phys.* **1998**, *109*, 3919.
(8) Zerda, T. W.; Wiegand, B.; Jonas, J. *J. Chem. Eng. Data* **1986**, *31*, 274.
(9) Zerda, T. W.; Xong, X.; Jonas, J. *Appl. Spectrosc.* **1986**, *40*, 1194.
(10) Gupta, S. K.; Lesslie, R. D.; King, A. D., Jr. *J. Phys. Chem.* **1973**, *77*, 2011
(11) Hemmaplardh, B.; King, A. D. *J. Phys. Chem.* **1972**, *76*, 2170.
(12) Kazarian, S. G.; Vincent, M. F.; Bright, F. V.; Liotta, C. L.; Eckert, C. A. *J. Am. Chem. Soc.* **1996**, *118*, 1729.
(13) Kollman, P. A. *J. Am. Chem. Soc.* **1977**, *99*, 4875.
(14) Peterson, K. I.; Klemperer, W. *J. Chem. Phys.* **1984**, *80*, 2439.
(15) Leopold, K. R.; Fraser, G. T.; Klemperer, W. *J. Am. Chem. Soc.* **1984**, *106*, 897.
(16) Nxumalo, L. M.; Ford, T. A.; Cox, A. J. *J. Mol. Struct.* **1994**, *307*, 153.
(17) Nxumalo, L. M.; Ford, T. A. *J. Mol. Struct.* **1994**, *327*, 145.
(18) Eckert, C. A.; Knutson, B. L.; Debenedetti, P. G. *Nature (London)* **1996**, *383*, 313.
(19) Brennecke, J. F. *Nature (London)* **1997**, *389*, 333.
(20) Kazarian, S. G. *Polym. Sci., Ser. C* **2000**, *42*, 78.
(21) Ventosa, N.; Sala, S.; Vecciana, J. *Cryst. Growth Des.* **2001**, *1*, 299.
(22) Lalanne, P.; Rey, S.; Cansell, F.; Tassaing, T.; Besnard, M. *J. Supercrit. Fluids* **2001**, *19*, 199.
(23) Poliakoff, M.; Howdle, S. M.; Kazarian, S. G. *Angew. Chem., Int. Ed. Engl.* **1995**, *34*, 1275.
(24) Kazarian, S. G.; Gupta, R. B.; Clarke, M. J.; Johnston, K. P.; Poliakoff, M. *J. Am. Chem. Soc.* **1993**, *115*, 11099.
(25) Fulton, J. L.; Yee, G. G.; Smith, R. D. *J. Am. Chem. Soc.* **1991**, *113*, 8327.
(26) Reilly, J. T.; Bokis, C. P.; Donohue, M. D. *Int. J. Thermophys.* **1995**, *16*, 599.
(27) Lalanne, P. Ph.D. Thesis. Université Bordeaux I, Bordeaux, France, 2001.
(28) Frisch, M. J.; Trucks, G. W.; Schlegel, H. B.; Scuseria, G. E.; Robb, M. A.; Cheeseman, J. R.; Zakrzewski, V. G.; Montgomery, J. A., Jr.; Stratmann, R. E.; Burant, J. C.; Dapprich, S.; Millam, J. M.; Daniels, A. D.; Kudin, K. N.; Strain, M. C.; Farkas, O.; Tomasi, J.; Barone, V.; Mennucci, B.; Cossi, M.; Adamo, C.; Jaramillo, J.; Cammi, R.; Pomelli, C.; Ochterski, J.; Petersson, G. A.; Ayala, P. Y.; Morokuma, K.; Malick, D. K.; Rabuck, A. D.; Raghavachari, K.; Foresman, J. B.; Ortiz, J. V.; Cui, Q.; Baboul, A. G.; Clifford, S.; Cioslowski, J.; Stefanov, B. B.; Liu, G.; Liashenko, A.; Piskorz, P.; Komaromi, I.; Gomperts, R.; Martin, R. L.; Fox, D. J.; Keith, T.; Al-Laham, M. A.; Peng, C. Y.; Nanayakkara, A.; Challacombe, M.; Gill, P. M. W.; Johnson, B.; Chen, W.; Wong, M. W.; Andres, J. L.: Gonzalez, C.; Head-Gordon, M.; Replogle, E. S.; Pople, J. A. *Gaussian 99*, Development Version, revision C.01; Gaussian, Inc.: Pittsburgh, PA, 2000.
(29) Moller, C.; Plesset, M. S. *Phys. Rev.* **1934**, *46*, 618.
(30) Pulay, P. *J. Comput. Chem.* **1982**, *3*, 556.
(31) Dunning, T. H. *J. Chem. Phys.* **1989**, *90*, 551.
(32) Wilson, A. K.; Mourik, T. V.; Dunning, T. H. *J. Mol. Struct.* **1996**, *388*, 339.
(33) Tatewaki, H.; Huzinaga, S. *J. Comp. Chem.* **1980**, *3*, 205.
(34) Kendall, R. A.; Dunning, T. H., Jr.; Harrison, R. J. *J. Chem. Phys.* **1992**, *96*, 6796.
(35) Boys, S. F.; Bernardi, F. *Mol. Phys* **1970**, *19*, 553.
(36) Wilson, E. B.; Decius, J. C.; Cross, P. C. *Molecular Vibrations*; McGraw-Hill: New York, 1955.
(37) Fredericks, S. Y.; Jordan, K. D.; Zwier, T. S. *J. Phys. Chem.* **1996**, *100*, 7810.
(38) Tarakeshwar, P.; Kim, K. S.; Brutschy, B. *J. Chem. Phys.* **1999**, *110*, 8501.
(39) Tarakeshwar, P.; Kim, K. S.; Brutschy, B. *J. Chem. Phys.* **2000**, *112*, 1769.
(40) Tarakeshwar, P.; Choi, S. C.; Lee, S. J.; Kim, K. S.; Ha, T. K.; Yang, J. H.; Lee, J. G.; Lee, H. *J. Chem. Phys.* **1999**, *111*, 5838.
(41) Rauhut, G.; Azhary, A. E.; Eckert, F.; Schumann, U.; Werner, H. J. *Spectrochim. Acta, Part A* **1999**, *55*, 647.
(42) Pophristic, V.; Goodman, L. *J. Phys. Chem. A* **2002**, *106*, 1642.
(43) Senent, M. L.; Domiguez-Gomez, R.; Villa, M. *J. Chem. Phys.* **2000**, *112*, 5809.
(44) Besnard, M.; Tassaing, T.; Danten, Y. Unpublished data.